Published in final edited form as:
Brain Behav Immun. 2015 February ; 44: 91–99. doi:10.1016/j.bbi.2014.08.010.

Spinal neuroimmmune activation is independent of T-cell infiltration and attenuated by A3 adenosine receptor agonists in a model of oxaliplatin-induced peripheral neuropathy

Kali Janes[a], **Carrie Wahlman**[a], **Joshua W. Little**[a], **Timothy Doyle**[a], **Dillip K. Tosh**[b], **Kenneth A. Jacobson**[b], and **Daniela Salvemini**[a,§]

[a]Department of Pharmacological and Physiological Science, Saint Louis University School of Medicine, 1402 South Grand Blvd, St. Louis, MO 63104, USA

[b]Molecular Recognition Section, Laboratory of Bioorganic Chemistry, National Institute of Diabetes and Digestive and Kidney Diseases, National Institutes of Health, Bethesda, MD 20892-0810, USA

Abstract

Many commonly used chemotherapeutics including oxaliplatin are associated with the development of a painful chemotherapy-induced peripheral neuropathy (CIPN). This dose-limiting complication can appear long after the completion of therapy causing a significant reduction in quality-of-life and impeding cancer treatment. We recently reported that activation of the G_i/G_q-coupled A_3 adenosine receptor (A_3AR) with selective A_3AR agonists (i.e., IB-MECA) blocked the development of chemotherapy induced-neuropathic pain in models evoked by distinct agents including oxaliplatin without interfering with their anticancer activities. The mechanism(s) of action underlying these beneficial effects has yet to be explored. Our results demonstrate that the development of oxaliplatin-induced mechano-hypersensitivity (allodynia and hyperalgesia) in rats is associated with the hyperactivation of astrocytes, but not microglial cells, increased production of pro-inflammatory and neuroexcitatory cytokines (TNF, IL-1β), and reductions in the levels of anti-inflammatory/neuroprotective cytokines (IL-10, IL-4) in the dorsal horn of the spinal cord. These events did not require lymphocytic mobilization since oxaliplatin did not induce $CD45^+/CD3^+$ T-cell infiltration into the spinal cord. A_3AR agonists blocked the development of neuropathic pain with beneficial effects strongly associated with the modulation of spinal neuroinflammatory processes: attenuation of astrocytic hyperactivation, inhibition of TNF and IL-1β production, and an increase in IL-10 and IL-4. These results suggest that inhibition of an astrocyte-associated neuroinflammatory response contributes to the protective actions of A_3AR

§Corresponding author: salvemd@slu.edu, Phone: 1-314-977-6430, Fax: 1-314-977-6441, Address: 1402 South Grand Blvd, St. Louis, MO 63104, USA.

The authors claim no conflicts of interest.

signaling and continues to support the pharmacological basis for selective A_3AR agonists as adjuncts to chemotherapeutic agents for the management of chronic pain.

Keywords

adenosine; A3 adenosine receptor; neuroinflammation; chemotherapy-induced peripheral neuropathy; neuropathic pain; oxaliplatin; astrocytes; spinal cord

1. Introduction

Oxaliplatin, a third generation platinum compound used for the treatment of metastatic colorectal cancer, is hindered by the dose-limiting development of chemotherapy-induced peripheral neuropathy (CIPN) accompanied by chronic neuropathic pain (1, 2). The primarily sensory symptoms occur in up to 60% of patients and commonly have a delayed manifestation that can linger for years (3, 4). Unfortunately, these patients suffer from both the physical symptoms and a decreased quality-of-life (1, 5). Critically, according to the American Society of Clinical Oncology no agents are currently recommended to either prevent or treat CIPN (6) and unfortunately, current pain drugs only offer marginal relief due to either a lack of efficacy or the risk of unacceptable side effects (1).

The purine nucleoside adenosine generated in both intra- and extracellular spaces by almost all cell types (7) has been shown to play an important role in many processes including pain (8, 9). In response to stress or injury, the extracellular concentration of adenosine can increase up to 1000-fold (10) and elicit responses in various cell types of the central nervous system including neurons, astrocytes, and microglia (9). Adenosine signaling is mediated by a family of G protein-coupled adenosine receptors (ARs): A_1, A_{2A}, A_{2B}, and A_3. The receptor subtypes are distinguishable by the G_α subunit they bind: A_1 and A_3 are coupled to G_i proteins while A_{2A} and A_{2B} are coupled to G_s (11). Adenosine provides potent and long-lasting pain relief in both preclinical animal models and human subject studies (12, 13); however, effective targeting of this endogenous pathway for the management of pain remains elusive (12). While adenosine's analgesic effect has primarily been attributed to A_1AR and to a lesser extent A_{2A}AR activation (12), these assumptions were made without consideration of A_3AR's contribution. Consequently, the focus of preclinical and clinical research over the past decade has been on the use of A_1AR/A_{2A}AR agonists for the treatment of chronic pain. These efforts have thus far proven unsuccessful in yielding a usable therapeutic option owing to several undesirable consequences, notably, cardiovascular side effects due to A_1AR/A_{2A}AR activation (12, 14). We recently reported that endogenous adenosine signals via A_3AR to inhibit chronic neuropathic pain (15) and have identified selective orally bioavailable A_3AR agonists as potent non-narcotic analgesics across several preclinical models of chronic neuropathic pain, including CIPN (16). Contrasting A_1AR and A_{2A}AR agonist's restricted therapeutic use, A_3AR agonists, including IB-MECA, have already advanced to phase II/III clinical trials for non-pain states and have thus far displayed good safety profiles (17, 18). While we have identified that A_3AR agonists reverse mechano-hypersensitivities through the activation of A_3ARs in regions responsible for nociceptive processing (i.e., the spinal cord and rostral ventromedial medulla (15), the signaling pathways engaged at these sites remain unknown.

Dysfunction in neuro-glial communication plays a key role in neuropathic pain of various etiologies (19–21), including neuropathic pain induced by paclitaxel (22–24), oxaliplatin (25, 26), and vincristine (27). This dysfunction arises from the development of neuroimmune activation (e.g., the activation of glia and increased glial-derived pro-inflammatory cytokine production) resulting in modified neurotransmission (e.g., excessive activation of glutamate receptors) within the spinal cord dorsal horn. Other possible sources of pro-inflammatory cytokines and potential drivers of neuropathic hypersensitivity are T-cells (Th17, Th1). The migration of pro-inflammatory T-cells into the spinal cord has been implicated in the development of hypersensitivity in several pain models including chronic constriction injury (CCI) (28) and spinal nerve ligation (29). However, it is unknown whether T-cell infiltration into the spinal cord also contributes to oxaliplatin-induced neuropathic pain.

A_3AR is highly expressed in several inflammatory cells, including glial cells (30–32) and T-cells (33), and its activation has been shown to suppress pro-inflammatory cytokine production in models of colitis, septic peritonitis, and rheumatoid arthritis (34–36). In this study, we examined whether A_3AR agonists block mechano-hypersensitivity in a model of oxaliplatin-induced neuropathic pain by inhibiting spinal neuroinflammatory processes.

2. Materials and Methods

2.1 Experimental animals

Male Sprague Dawley rats (200–220 g starting weight) from Harlan Laboratories (Indianapolis, IN; Frederick, MD breeding colony) were housed 3–4 per cage in a controlled environment (12 h light/dark cycle) with food and water available *ad libitum*. All experiments were performed in accordance with the International Association for the Study of Pain and the National Institutes of Health guidelines on laboratory animal welfare and the recommendations by Saint Louis University Institutional Animal Care and Use Committee. All experiments were conducted with the experimenters blinded to treatment conditions.

2.2 Test Compounds

In prophylactic paradigms, all IB-MECA and MRS5698 were given 15–20 min prior to oxaliplatin (D0–4). When used, MRS1523 was administered 15–20 minutes before IB-MECA or MRS5698. IBMECA (1-deoxy-1-[6-[[(3-iodophenyl)methyl]amino]-9*H*-purin-9-yl]-*N*-methyl-β-D-ribofuranuronamide) was purchased from Tocris Bioscience (Bristol, United Kingdom). MRS1523 (3-propyl-6-ethyl-5-[(ethylthio)carbonyl]-2-phenyl-4-propyl-3-pyridine-carboxylate) was obtained from Sigma-Aldrich (St. Louis, MO). MRS5698 (1*S*,2*R*,3*S*,4*R*,5*S*)-4-(6-((3-chlorobenzyl)amino)-2-((3,4-difluorophenyl) ethynyl)-9*H*-purin-9-yl)-2,3-dihydroxy-*N*-methylbicyclo[3.1.0]hexane-1-carboxamide was synthesized as previously described (37).

2.3 Oxaliplatin-induced neuropathic pain model

Oxaliplatin (Oncology Supply; Dothan, AL) or its vehicle (5% dextrose) was injected by intraperitoneal (i.p.) injection in rats on 5 consecutive days (D0–4) at an injection volume of

0.2 ml for a final cumulative dose of 10 mg/kg. This low dose paradigm does not cause kidney injury, as previously reported by Bennett's lab (38).

2.4 Behavioral testing

Behavioral measurements to assess mechano-hypersensitivity were always taken prior to the administration of test substances. Mechano-allodynia was measured as previously described (22, 24). Briefly, rats were allowed to acclimate to behavioral chambers for 15 min prior to measuring the mechanical paw withdrawal thresholds, grams [PWT, (g)] by an electronic Von Frey test (dynamic plantar aesthesiometer, model 37450; Ugo Basile, Italy) with a cut off set at 50 g. Mechano-allodynia was defined by a significant ($P<0.05$) reduction in mechanical mean absolute PWT (g) at forces that failed to elicit withdrawal responses before chemotherapy treatment (D0). Mechano-hyperalgesia was measured by stimulating the dorsum of the rat's hind paw as previously described (22, 24) by the Randall and Sellitto paw pressure test (40) using a Ugo-Basile analgesiometer (Italy, model 37215). The nociceptive paw withdrawal threshold [PWT, (g)] was defined as the force (g) which caused the rat to withdraw its paw (cut off set at 250 g). Since, chemotherapy-induced neuropathy results in bilateral allodynia and hyperalgesia with no differences between left and right hind PWT (g), the values from both paws were averaged. Animals receiving chemotherapeutic agents in the presence or absence of the experimental test substances tested did not display signs of any toxicities, as previously described (38, 41).

2.5 Multiplex Cytokine Assay

The levels of cytokines in spinal cord (L4–6) lysates were either assessed using a commercially available, custom-ordered magnetic multiplex cytokine kit (Bio-Rad Laboratories; Hercules, CA) as previously described (22).

2.6 Immunofluorescence

Immunofluorescence was performed using modifications of previously reported methods (42). After behavioral measurements, rats were sacrificed according to SLU IACUC regulations. The lower lumbar enlargement of the spinal cord (L4–L6) was harvested, transferred to OCT, and frozen in an isopropanol/dry ice bath. Transverse sections (20 μm) were cut using a cryostat, collected on gelatin coated glass microscope slides, and stored at −20 °C. Spinal cord sections were fixed in 10% buffered neutral formalin (10 min), blocked (10% normal goat serum, 2% bovine serum albumin, 0.2% Triton-X100 in phosphate buffered saline, PBS, for 1 h) then immunolabeled as previously described (42) using an 18 h incubation (4°C) with mouse monoclonal anti-glial fibrillary acidic protein (GFAP) antibody (1:200; Sigma-Aldrich) or OX42 antibody (CD11b antigen, 1:50; Millipore). Following a series of PBS rinses, sections were incubated for 2 h with a goat anti-mouse Alexa Fluor 488 antibody (1:250; Invitrogen). The coverslips were mounted with Fluorogel II containing DAPI (Electron Microscopy Sciences; Hatfield, PA) and photographed with an Olympus FV1000 MPE confocal microscope (multiline argon lasers with excitation at 405 nm and 488 nm) using a 10X objective (UPLSAPO; 0.4 NA) for regional fluorescence intensity image analysis and with a 60X oil-immersion objective (PLAPONl 1.42 NA) and 2.4X optical zoom (0.1 μm pixel dimensions in the X-Y plane and the pinhole set at 1 Airy unit) for higher magnification images. Images were acquired within the dynamic range of

the microscope (i.e., no pixel intensity values of 0 or 255 in an 8-bit image). Sections treated with isotype controls at equivalent concentrations to primary antibodies yielded only non-specific background fluorescence. The mean fluorescence intensity (MFI) in the dorsal horn was determined as previously reported (42). Image analysis was performed using the NIH freeware program ImageJ (version 1.43) (43). The superficial dorsal horns (laminae I and II) at the L4, L5, and L6 levels were outlined on images bilaterally using the Image J region of interest tool. The superficial dorsal horn was determined and confirmed using cresyl violet stained sections of adjacent sections and an atlas (44). There were no significant differences bilaterally, so MFI was calculated as a combined value and reported as fold change compared to the vehicle group.

2.7 Quantitative RT-PCR

Terminally anesthetized rats were perfused with cold PBS (pH 7.4). The L4/L5 spinal cord dorsal horn and dorsal root ganglion were harvested and placed in RNA*later* (Sigma-Aldrich). RNA was extracted from tissue by Qiagen RNeasy Plus Universal Kit (Valencia, CA) and reverse transcribed following manufacturer's instructions. The relative transcript expression of CD4 and HPRT1 were measured using SYBR green-based quantitative real-time PCR and commercial CD4 and HPRT1 primers (Qiagen) (29). The fold change in oxaliplatin-treated over vehicle-treated rats was calculated using the comparative Ct method with HPRT1 used as the endogenous control (45).

2.8 Flow cytometry

The $CD45^+/CD3^+$ T-cell population was measured in the contralateral and ipsilateral spinal cord from rats subjected to sham/CCI-surgery or in the bilateral dorsal horns of rats treated with vehicle or oxaliplatin. Rats were transcardially perfused with 200 ml of cold PBS (pH 7.4) and the lumbar enlargement (L4–L6) harvested. The meninges were removed from the spinal cord to eliminate leukocytes that may have adhered to the small blood vessels of the meninges after perfusion. Although these cells may play a role if present, they were not the focus of this study. Spinal cords were bisected into contralateral and ipsilateral (CCI) or dorsal and ventral halves (CIPN). Each spinal cord sample was mechanically and enzymatically dissociated, then purified as previously described (46). Briefly, samples were minced in cold Dulbecco's minimal essential media (DMEM, Sigma-Aldrich) and enzymatically digested in trypsin (0.5 mg/ml, Sigma-Aldrich) and collagenase (1 mg/ml, Sigma-Aldrich) for 20 minutes at 37°C. The tissues were triturated with an 18 gauge needle and 10 ml of DMEM + 10% fetal bovine serum was added to stop the enzymatic digestion. The homogenate was passed through a 40 μm nylon mesh (BD Biosciences), centrifuged (1000 x g, 5 min), and the pellet resuspended in Hank's balanced salt solution (HBSS) (Sigma-Aldrich). Myelin was removed by Optiprep gradient in HBSS prepared as previously described (46) and centrifuged for 20 min at 726 x g at RT without brake. The top fraction (8 ml) containing myelin was removed. The remaining solution was collected and washed twice in HBSS. The entire purified single-cell pellet was then resuspended in HBSS and transferred to a 12 × 75 mm Falcon (BD Biosciences) polystyrene tube. The tubes were centrifuged and the pellets blocked in PBS (pH 7.4) with 5% normal mouse serum (Sigma-Aldrich) and anti-CD32 (1:500, BD Bioscience) for 30 min at RT. After removing the blocking buffer the pellet was suspended in 100 μL of antibody cocktail

[mouse anti-rat CD45-APC (0.25μg/tube; eBioscience), mouse anti-rat CD3-PE (0.1 μg/tube; eBioscience) in blocking buffer] or IgG cocktail [mouse $IgG_{1\kappa}$-APC (0.25 μg/tube; eBioscience), mouse IgG_3-PE (0.1 μg/tube) in blocking buffer]. The tubes were incubated for 30 min at RT, washed twice in PBS, and fixed in 4% formalin in PBS (pH 7.4). As a control, the remaining upper lumbar and cervical sections of two rats were collected and similarly processed. One control tissue was spiked before digestion with 100 μl of pooled whole blood obtained from tail vein withdrawals from each rat to assess recovery and detection of $CD45^+/CD3^+$ cells. The gates for flow cytometry were set using whole blood (100 μL) stained for CD45, CD3, or both. These blood samples (100 μl) were blocked for 30 min at RT then stained with anti-CD45-APC, anti-CD3-PE, or antibody cocktail for 30 min after which they were fixed in 4% formalin in PBS. Red blood cells from spiked spinal cord and whole blood samples were lysed using previously described method with slight modification (47): after staining and formalin-fixing, cells were treated with 0.2% Triton X-100 in PBS for 30 min at 4°C instead of 10 min at 37°C to lyse red blood cells.

The samples were read using two-color flow cytometric analysis by a BD LSR II flow cytometer (BD Biosciences). The lasers and filter used were 635 nm and 488 nm excitation and 660/20 nm and 575/26 nm emission filter for APC and PE, respectively. To ensure the detection of low T-cell numbers with our flow analysis, the entire spinal cord sample was read ($\leq 10^6$ events) and the gates were set using whole blood (5×10^4–1×10^5 events) and spiked spinal cord samples ($\leq 10^6$ events). The first gate [side scatter (SSC) vs. forward scatter-all (FSC-A)] was set to reduce the number of debris and myelin (Supplemental Fig. 1A). Singlets were isolated by using the second gate [forward-scatter-height (FSC-H) vs. FSC-A] (Supplemental Fig. 1B). The $CD45^+$ population was separated by a third gate [FSC-A vs. CD45-APC of the singlet population] (Supplemental Fig. 1C). Finally, the $CD3^+$ population in the $CD45^+$ population was gated [FSC-A vs. CD3-PE of the $CD45^+$ population] (Supplemental Fig. 1D). The ability to recover and detect CD45+/CD3+ cells following these methods and gates was confirmed in spinal cords (C3-L3) with or without a spike of 100 μl whole blood (Supplemental Fig. 1E–H). The frequency of $CD45^+/CD3^+$ cells is expressed as a percentage of the singlet cell population.

2.9 Statistical Analysis

Data are expressed as mean ± SD for n animals. The data from behavioral studies were analyzed by two-way repeated measures ANOVA with Bonferroni-corrected comparisons or one-way ANOVA with Dunnett's-corrected comparisons as noted. All biochemical data collected on D25 were analyzed by one-way ANOVA with Dunnett's-corrected comparisons or by Student's t-test. Significant differences were defined as $P<0.05$. All statistical analyses were performed using GraphPad Prism (v5.03, GraphPad Software, Inc.).

3. Results

3.1 A_3AR agonists prevent oxaliplatin-induced neuropathic pain

Consistent with previous studies (38), including our own (16, 41), a five day (D) treatment with oxaliplatin (D0–4) produced a time-dependent development of mechano-allodynia and mechano-hyperalgesia (mechano-hypersensitivity) as evidenced by a significant decrease in

paw withdrawal thresholds (PWTs (g)) beginning on D11 (onset) and reaching a peak by D17 that continued through the end of our observation period (D25; times relative to first injection) (Fig. 1A, B; *n=5*). As with patients, this rat model displays a delay to the onset of mechano-hypersensitivity mimicking the clinical "coasting" phenomenon observed with patients (1, 2). We recently reported that daily (D0–16) i.p. delivery of IB-MECA dose-dependently attenuated mechano-allodynia and mechano-hyperalgesia with ED_{50}s on D17 of 0.026 mg/kg and 0.031 mg/kg respectively (16). Using a dose of IB-MECA previously shown to cause near to maximal inhibition of mechano-hypersensitivity (0.1 mg/kg/d, (16)), we now examined whether restricting the dosing regimen of the A_3AR agonist IB-MECA to coincide with only the oxaliplatin treatment would afford the same protection as dosing patients only when they receive the chemotherapeutic agent would be a preferred regimen. IB-MECA (0.1 mg/kg/d, *n=5*) when given 20 minutes prior to oxaliplatin (D0–4), blocked the development of neuropathic pain through D25 (Fig. 1A, B).

While IB-MECA exhibits exquisite selectivity (>50-fold) for the rat and human A_3AR subtype over the other AR subtypes (48, 49), we employed an A_3AR agonist with an even higher selectivity, MRS5698, (16) in order to strengthen our findings. MRS5698 has a very high affinity for A_3AR (≤3 nM) and excellent selectivity (≥10^4-fold over human and mouse A_1AR or A_{2A}AR) (37). Similar to our above findings with IB-MECA, co-administration of MRS5698 (0.1 mg/kg/d, *n=6*) with oxaliplatin blocked the development of mechano-hypersensitivity (Fig. 2A, B). MRS5698 (*n=5*) had no effect on the PWTs of vehicle-treated animals (Fig. 2A, B).

The beneficial actions of IB-MECA and MRS5698 were prevented by the selective A_3AR antagonist, MRS1523 (50), confirming an A_3AR-mediated mechanism of action. MRS1523 (2 mg/kg/d, *n=5*) was given by i.p. injection 15–20 minutes prior to IB-MECA or MRS5698 on D0–4 of oxaliplatin-treatment. MRS1523 had no effect when given on its own to oxaliplatin-treated animals (Fig. 3; *n=5*). As published in our previous paper with another model of CIPN (paclitaxel), MRS1523 given to vehicle-treated animals had no effect on PWTs (16). Thus, in an effort to eliminate unnecessary animal usage, we did not include a vehicle + MRS1523 group in this study.

3.2 A_3AR agonists prevent astrocytic hyperactivation and increase pro-inflammatory cytokine production in the spinal cord

Neuroinflammation (enhanced glial activation and pro-inflammatory cytokine production) in the spinal cord is a key contributor to the development of central sensitization associated with pain of several etiologies, including oxaliplatin-induced pain (22, 23, 51). Activation of astrocytes and microglia was assessed by immunofluorescence utilizing antibodies directed against GFAP and OX42 respectively. When compared to their vehicle-treated counterparts oxaliplatin-treated rats at the same time-point demonstrated enhanced bilateral immunolabeling of GFAP (Fig. 4E–K), but not OX42 (Fig. 4A–D) within the superficial dorsal horn (i.e., laminae I & II) in agreement with previously published findings (52). This increased GFAP labeling was absent in spinal cords from animals receiving MRS5698 in combination with oxaliplatin (Fig. 4G, K).

Additionally, oxaliplatin-treatment coincided with an alteration in the levels of pro-/anti-inflammatory cytokines within the spinal cord. The levels of TNF (formerly known as TNF-α) and IL-1β (Fig. 5A, B; *n=6*) were significantly increased, whereas the anti-inflammatory IL-10 and IL-4 (Fig. 5C, D; *n=6*) were slightly decreased as compared to levels in their vehicle-treated counterparts. Prophylactic treatment with either IB-MECA or MRS5698 reduced the production of the pro-inflammatory TNF and IL-1β to vehicle levels and significantly increased the production of the anti-inflammatory IL-10 and IL-4 (Fig. 5; *n=6*). Conversely, these beneficial effects of IB-MECA and MRS5698 were blocked by pretreatment with the A_3AR antagonist MRS1523 (Fig. 5; *n=5*). As there was no change in the PWTs of oxaliplatin animals treated with MRS1523 and in an effort to reduce animal usage, we did not investigate the cytokine expression in this group.

3.3 T-cell infiltration into the spinal cord does not occur in response to oxaliplatin-treatment

The level of T-cell infiltration into the lumbar spinal cord (L4–L6) after oxaliplatin treatment was measured by qRT-PCR for CD4 expression levels and flow cytometric analysis of $CD45^+/CD3^+$ T-cell populations. At the plateau of mechano-hypersensitivity (D25), there were no significant changes in the expression of $CD4^+$ transcript (Table 1) or $CD45^+/CD3^+$ cells (Fig. 6; *n=5*) in the dorsal lumbar spinal cord of oxaliplatin-treated animals when compared to vehicle; this was also observed at earlier time points (D0, D5, D11, and D17; data not shown). In order to rule out the lack of effect from methodological issue, we assessed T-cell infiltration in spinal cord following nerve-injury evoked mechano-hypersensitivity caused by CCI of the sciatic nerve in rats (42, 53). Previous studies showed that at seven days post-surgery (the peak development of mechano-allodynia) there is a significant increase of $CD4^+$ and $CD3^+$ cells in the ipsilateral (injured) side of the lumbar spinal cord as compared to the contralateral side (29, 54). Indeed, in the chronic constriction injury model we found a significant 4.5-fold increase in $CD45^+/CD3^+$ T-cell infiltration into the ipsilateral lumbar spinal cord when compared to the contralateral side at D7 post-surgery (data not shown).

4. Discussion

Oxaliplatin-induced neuropathic pain represents a major obstacle to successful cancer treatment as it restricts both individual and cumulative dosages. However, even with these limitations, patients are still forced to risk the development of long-lasting consequences (i.e., peripheral neuropathy) in order to optimize cancer therapies (1, 5). Further research is therefore necessary to fill the void currently present in adequate therapeutic options for the treatment of CIPN. With this in mind, two selective A_3AR agonists were chosen to investigate potential spinal signaling pathways through which they may exert their beneficial effects in a model of oxaliplatin-induced neuropathic pain: IB-MECA and MRS5698. Herein, we confirm our previous findings that activation of A_3AR by IB-MECA prevents the development of mechano-hypersensitivity in a rat model of oxaliplatin-induced neuropathic pain (16) and extend our findings with the highly selective MRS5698. Noteworthy, the beneficial effects seen with IB-MECA were reproducible with MRS5698 indicating that these results are not particular to an agent or to nonspecific AR activation but

are rather due to agonism of the A_3 receptor subtype. Supporting this, pretreatment with the A_3AR antagonist MRS1523 mitigates the beneficial effects of IB-MECA and MRS5698. As patient compliance is always a concern in the clinical setting, our data using a different paradigm establishes that concomitant dosing of an A_3AR agonist delivers the same result as the longer term dosing we previously employed (16).

In an effort to understand the underlying pathological processes responsible for this prevention, we turned our attention to the spinal cord, a key center for nociceptive processing. A well-established hallmark of CIPN independent of the chemotherapeutic mechanism of action is the development of pathophysiological changes in the spinal cord as evidenced by neuroinflammatory processes including enhanced glial response and the release of pro-inflammatory cytokines (23, 26). Previous work examining the dorsal horn of oxaliplatin-treated animals supports the presence of glial hyperactivation evidenced by heightened staining for astrocytes (GFAP) through the end of testing (21 days), while increased microglia expression (Iba1) was only observed at early time-points (7 days) before resolving (52). Our findings at 25 days following the start of oxaliplatin treatment further support a key role for astrocytes in the maintenance of CIPN-induced neuropathic pain. During an enhanced response state, glial cells can release pro-inflammatory cytokines and nitroxidative species including superoxide and nitric oxide (19, 55). Indeed, in another model of chemotherapy (i.e., paclitaxel)-induced neuropathic pain, increased formation of pro-inflammatory cytokines was observed in the spinal cord (22). These pro-inflammatory events have long been associated with the development of pain of several etiologies including that due to peripheral inflammation, peripheral nerve trauma, or spinal cord injury (19, 22, 56). In addition to their supportive role in neuronal health, glial cells strongly influence neuronal signaling owing to their regulation of the uptake or release of neuroactive substances including, importantly, pro-inflammatory cytokines (21, 56). Once released, pro-inflammatory cytokines such as TNF and IL-1β can act not only on neurons resulting in enhanced excitability, but can also feedback on glial cells leading to an amplification loop that could potentially be responsible for the long-lasting hypersensitivity (56, 57). As it has already been established that oxaliplatin-treatment is linked with the development of astrocytic hyperactivation, we aimed to investigate whether intervention with an A_3AR agonist would mediate its beneficial actions via attenuation of neuroinflammation. Indeed, treatment with an A_3AR agonist prevented the oxaliplatin-associated 1) increased levels of astrocyte-associated GFAP and 2) production of pro-inflammatory cytokines TNF and IL-1β. Additionally, production of the anti-inflammatory cytokines IL-10 and IL-4 were enhanced after A_3AR administration. Giving further support to a solely A_3AR-mediated action, the selective A_3AR antagonist MRS1523 prevented the beneficial actions of IB-MECA and MRS5698 on cytokine production. While the exact mechanisms behind A_3AR's anti-inflammatory effects are unknown, it is possible that the A_3AR agonists prevent astrocytic hyperactivation through the inhibition of glycogen synthase kinase 3β (GSK3β). Increased activation of GSK3β in the spinal cord is associated with paclitaxel-induced pain and its inhibition attenuated elevated levels of GFAP and IL-1β in the spinal cord (58). Furthermore, Fishman and associates demonstrated that suppression of colon carcinoma growth *in vitro* by IB-MECA was attributed to GSK3β inhibition (59). Additionally, A_3AR's protection against mitochondrial dysfunction during ischemia/reperfusion injury is attributed

at least in part to the inactivation of GSK3β via the phosphatidylinositol 3-kinase/protein kinase B (Akt) signaling pathway (60) giving a positive indication that A_3AR may also protect against the mitochondrial dysfunction associated with oxaliplatin-induced pain. A_3AR agonists have also been shown to reduce pro-inflammatory cytokines by inhibiting the p38 mitogen activated protein kinases and nuclear factor κB signaling pathways (61–63); this may also hold true for oxaliplatin-induced neuropathic pain. (64, 65). Although unknown, our laboratories are currently investigating the cellular source(s) of the increased anti-inflammatory cytokine production underlying CIPN.

In other models of neuropathic pain including CCI and spinal nerve ligation, infiltration of circulating T-cells from the periphery into the spinal cord contributes to neuroinflammation and the development of hypersensitivity (29, 54, 66). In fact, intraperitoneal passive transfer of polarized pro-inflammatory Th1 cells enhances CCI-induced neuropathy in nude mice, whereas, similar transfer of polarized anti-inflammatory Th2 cells in immunocompetent rats attenuates CCI-induced neuropathic pain (67). However, infiltration into the spinal cord during the development of oxaliplatin-induced neuropathic pain did not occur leading us to conclude that T-cell infiltration into the spinal cord does not play a part in the development of oxaliplatin-induced neuropathic pain. Although we find no additional T-cell infiltration, we did not further characterize the $CD4^+$ subtypes (i.e., Th1 vs. Th2) and therefore cannot exclude the possibility of $CD4^+$ T-cells "switching" from a pro-inflammatory (Th1) state to an anti-inflammatory (Th2) state (68) in response to IB-MECA or MRS5698. In an anti-inflammatory state, these cells could produce and release the potent anti-inflammatory cytokine, IL-10. Spinal formation of IL-10 may play a major role in A_3AR's beneficial actions as its activation is associated with increased formation of the anti-inflammatory cytokine (Figs. 3 and 5) and strategies aimed at increasing its production within the spinal cord have proven successful in a model of paclitaxel-induced neuropathic pain by decreasing the production of pro-inflammatory cytokines (i.e., TNF and IL-1) (69). The anticancer actions of A_3AR agonists on their own may be beneficial to these patients. Given that A_3AR density has been shown to be significantly increased in colon and breast carcinoma (2.3-fold higher) (70) and that A_3AR agonists have already been demonstrated to have direct anticancer actions both *in vitro* and *in vivo* (17, 71–73), a unique opportunity may exist. Our group has shown that *in vitro* anticancer actions of several classes of chemotherapeutics (i.e., platinum-based agents, taxanes, and proteasome inhibitors) remain unaffected in combination with IB-MECA treatment. (16). In light of this, A_3AR agonists could potentially provide added benefit by enhancing anti-cancer strategies when given in conjunction with chemotherapeutics.

Collectively, our study suggests that T-cell independent inhibition of an astrocytic hyperactivation and pro-inflammatory cytokine production within the spinal cord contributes to the protective actions of A_3AR signaling and continues to support the pharmacological basis for selective A_3AR agonists as adjuncts to chemotherapeutic agents for the management of chronic pain.

Supplementary Material

Refer to Web version on PubMed Central for supplementary material.

Acknowledgments

We would like to thank Leesa Bryant for her technical assistance in performing some of the animal experiments. This study was funded by grants from NCI with additional support from the Saint Louis Cancer Center, and the NIDDK Intramural Research Program.

Abbreviations

AR	adenosine receptor
CCI	chronic constriction injury
CIPN	chemotherapy-induced peripheral neuropathy
MFI	mean fluorescence intensity
PWT	paw withdrawal threshold

References

1. Farquhar-Smith P. Chemotherapy-induced neuropathic pain. Curr Opin Support Palliat Care. 2011; 5(1):1–7. [PubMed: 21192267]
2. Quasthoff S, Hartung HP. Chemotherapy-induced peripheral neuropathy. Journal of neurology. 2002; 249(1):9–17. [PubMed: 11954874]
3. Velasco R, Bruna J. Chemotherapy-induced peripheral neuropathy: an unresolved issue. Neurologia. 2010; 25(2):116–31. [PubMed: 20487712]
4. Argyriou AA, Polychronopoulos P, Iconomou G, Chroni E, Kalofonos HP. A review on oxaliplatin-induced peripheral nerve damage. Cancer Treat Rev. 2008; 34(4):368–77. [PubMed: 18281158]
5. Kannarkat G, Lasher EE, Schiff D. Neurologic complications of chemotherapy agents. Curr Opin Neurol. 2007; 20(6):719–25. [PubMed: 17992096]
6. Hershman DL, Lacchetti C, Dworkin RH, Lavoie Smith EM, Bleeker J, Cavaletti G, Chauhan C, Gavin P, Lavino A, Lustberg MB, et al. Prevention and management of chemotherapy-induced peripheral neuropathy in survivors of adult cancers: american society of clinical oncology clinical practice guideline. Journal of clinical oncology: official journal of the American Society of Clinical Oncology. 2014; 32(18):1941–67. [PubMed: 24733808]
7. Zimmermann H. Extracellular metabolism of ATP and other nucleotides. Naunyn Schmiedebergs Arch Pharmacol. 2000; 362(4–5):299–309. [PubMed: 11111825]
8. Chen JF, Eltzschig HK, Fredholm BB. Adenosine receptors as drug targets--what are the challenges? Nat Rev Drug Discov. 2013; 12(4):265–86. [PubMed: 23535933]
9. Fredholm BB, APIJ, Jacobson KA, Linden J, Muller CE. International Union of Basic and Clinical Pharmacology. LXXXI. Nomenclature and classification of adenosine receptors--an update. Pharmacol Rev. 2011; 63(1):1–34. [PubMed: 21303899]
10. Ballarin M, Fredholm BB, Ambrosio S, Mahy N. Extracellular levels of adenosine and its metabolites in the striatum of awake rats: inhibition of uptake and metabolism. Acta Physiol Scand. 1991; 142(1):97–103. [PubMed: 1877368]
11. Fredholm BB, APIJ, Jacobson KA, Klotz KN, Linden J. International Union of Pharmacology. XXV. Nomenclature and classification of adenosine receptors. Pharmacol Rev. 2001; 53(4):527–52. [PubMed: 11734617]
12. Zylka MJ. Pain-relieving prospects for adenosine receptors and ectonucleotidases. Trends Mol Med. 2011; 17(4):188–96. [PubMed: 21236731]
13. Hayashida M, Fukuda K, Fukunaga A. Clinical application of adenosine and ATP for pain control. Journal of anesthesia. 2005; 19(3):225–35. [PubMed: 16032451]
14. Boison D. Adenosine kinase: exploitation for therapeutic gain. Pharmacol Rev. 2013; 65(3):906–43. [PubMed: 23592612]

15. Little J, Chen Z, Ford A, Janes K, Doyle T, Tosh D, Jacobson K, Salvemini D. (297) Central adenosine A3 receptor (A3AR) activation reverses neuropathic pain. The journal of pain: official journal of the American Pain Society. 2014; 15(4):S50.
16. Chen Z, Janes K, Chen C, Doyle T, Bryant L, Tosh DK, Jacobson KA, Salvemini D. Controlling murine and rat chronic pain through A3 adenosine receptor activation. FASEB journal: official publication of the Federation of American Societies for Experimental Biology. 2012; 26(5):1855–65. [PubMed: 22345405]
17. Fishman P, Bar-Yehuda S, Liang BT, Jacobson KA. Pharmacological and therapeutic effects of A3 adenosine receptor agonists. Drug discovery today. 2012; 17(7–8):359–66. [PubMed: 22033198]
18. Stemmer SM, Benjaminov O, Medalia G, Ciuraru NB, Silverman MH, Bar-Yehuda S, Fishman S, Harpaz Z, Farbstein M, Cohen S, et al. CF102 for the treatment of hepatocellular carcinoma: a phase I/II, open-label, dose-escalation study. The oncologist. 2013; 18(1):25–6. [PubMed: 23299770]
19. Cao H, Zhang YQ. Spinal glial activation contributes to pathological pain states. Neurosci Biobehav Rev. 2008; 32(5):972–83. [PubMed: 18471878]
20. Obata K, Noguchi K. Contribution of primary sensory neurons and spinal glial cells to pathomechanisms of neuropathic pain. Brain Nerve. 2008; 60(5):483–92. [PubMed: 18516970]
21. Watkins LR, Milligan ED, Maier SF. Spinal cord glia: new players in pain. Pain. 2001; 93(3):201–5. [PubMed: 11514078]
22. Doyle T, Chen Z, Muscoli C, Bryant L, Esposito E, Cuzzocrea S, Dagostino C, Ryerse J, Rausaria S, Kamadulski A, et al. Targeting the overproduction of peroxynitrite for the prevention and reversal of paclitaxel-induced neuropathic pain. The Journal of neuroscience: the official journal of the Society for Neuroscience. 2012; 32(18):6149–60. [PubMed: 22553021]
23. Zhang H, Yoon SY, Dougherty PM. Evidence That Spinal Astrocytes but Not Microglia Contribute to the Pathogenesis of Paclitaxel-Induced Painful Neuropathy. J Pain. 2012
24. Janes K, Little JW, Li C, Bryant L, Chen C, Chen Z, Kamocki K, Doyle T, Snider A, Esposito E, et al. The Development and Maintenance of Paclitaxel-Induced Neuropathic Pain Requires Activation of the Sphingosine 1-Phosphate Receptor Subtype 1. The Journal of biological chemistry. 2014
25. Peters CM, Jimenez-Andrade JM, Kuskowski MA, Ghilardi JR, Mantyh PW. An evolving cellular pathology occurs in dorsal root ganglia, peripheral nerve and spinal cord following intravenous administration of paclitaxel in the rat. Brain research. 2007; 1168:46–59. [PubMed: 17698044]
26. Yoon SY, Robinson CR, Zhang H, Dougherty PM. Spinal astrocyte gap junctions contribute to oxaliplatin-induced mechanical hypersensitivity. J Pain. 2013; 14(2):205–14. [PubMed: 23374942]
27. Kiguchi N, Maeda T, Kobayashi Y, Saika F, Kishioka S. Involvement of inflammatory mediators in neuropathic pain caused by vincristine. International review of neurobiology. 2009; 85:179–90. [PubMed: 19607970]
28. Grace PM, Rolan PE, Hutchinson MR. Peripheral immune contributions to the maintenance of central glial activation underlying neuropathic pain. Brain, behavior, and immunity. 2011; 25(7): 1322–32.
29. Costigan M, Moss A, Latremoliere A, Johnston C, Verma-Gandhu M, Herbert TA, Barrett L, Brenner GJ, Vardeh D, Woolf CJ, et al. T-cell infiltration and signaling in the adult dorsal spinal cord is a major contributor to neuropathic pain-like hypersensitivity. The Journal of neuroscience: the official journal of the Society for Neuroscience. 2009; 29(46):14415–22. [PubMed: 19923276]
30. Poulsen SA, Quinn RJ. Adenosine receptors: new opportunities for future drugs. Bioorg Med Chem. 1998; 6(6):619–41. [PubMed: 9681130]
31. Ochaion A, Bar-Yehuda S, Cohen S, Barer F, Patoka R, Amital H, Reitblat T, Reitblat A, Ophir J, Konfino I, et al. The anti-inflammatory target A(3) adenosine receptor is over-expressed in rheumatoid arthritis, psoriasis and Crohn's disease. Cell Immunol. 2009; 258(2):115–22. [PubMed: 19426966]
32. Abbracchio MP, Rainaldi G, Giammarioli AM, Ceruti S, Brambilla R, Cattabeni F, Barbieri D, Franceschi C, Jacobson KA, Malorni W. The A3 adenosine receptor mediates cell spreading,

reorganization of actin cytoskeleton, and distribution of Bcl-XL: studies in human astroglioma cells. Biochem Biophys Res Commun. 1997; 241(2):297–304. [PubMed: 9425266]

33. Gessi S, Varani K, Merighi S, Cattabriga E, Avitabile A, Gavioli R, Fortini C, Leung E, Mac Lennan S, Borea PA. Expression of A3 adenosine receptors in human lymphocytes: up-regulation in T cell activation. Molecular pharmacology. 2004; 65(3):711–9. [PubMed: 14978250]
34. Szabó C, Scott GS, Virág L, Egnaczyk G, Salzman AL, Shanley TP, Haskó G. 1998
35. Mabley J, Soriano F, Pacher P, Hasko G, Marton A, Wallace R, Salzman A, Szabo C. The adenosine A3 receptor agonist, N6-(3-iodobenzyl)-adenosine-5′-N-methyluronamide, is protective in two murine models of colitis. Eur J Pharmacol. 2003; 466(3):323–9. [PubMed: 12694816]
36. Lee JY, Jhun BS, Oh YT, Lee JH, Choe W, Baik HH, Ha J, Yoon KS, Kim SS, Kang I. Activation of adenosine A3 receptor suppresses lipopolysaccharide-induced TNF-alpha production through inhibition of PI 3-kinase/Akt and NF-kappaB activation in murine BV2 microglial cells. Neurosci Lett. 2006; 396(1):1–6. [PubMed: 16324785]
37. Tosh DK, Deflorian F, Phan K, Gao ZG, Wan TC, Gizewski E, Auchampach JA, Jacobson KA. Structure-guided design of A(3) adenosine receptor-selective nucleosides: combination of 2-arylethynyl and bicyclo[3.1.0]hexane substitutions. Journal of medicinal chemistry. 2012; 55(10): 4847–60. [PubMed: 22559880]
38. Xiao WH, Zheng H, Bennett GJ. Characterization of oxaliplatin-induced chronic painful peripheral neuropathy in the rat and comparison with the neuropathy induced by paclitaxel. Neuroscience. 2012; 203:194–206. [PubMed: 22200546]
39. Dixon WJ. Efficient analysis of experimental observations. Annu Rev Pharmacol Toxicol. 1980; 20:441–62. [PubMed: 7387124]
40. Randall LO, Selitto JJ. A method for measurement of analgesic activity on inflamed tissue. Arch Int Pharmacodyn Ther. 1957; 111(4):409–19. [PubMed: 13471093]
41. Janes K, Doyle T, Bryant L, Esposito E, Cuzzocrea S, Ryerse J, Bennett GJ, Salvemini D. Bioenergetic deficits in peripheral nerve sensory axons during chemotherapy-induced neuropathic pain resulting from peroxynitrite-mediated post-translational nitration of mitochondrial superoxide dismutase. Pain. 2013; 154(11):2432–40. [PubMed: 23891899]
42. Little JW, Chen Z, Doyle T, Porreca F, Ghaffari M, Bryant L, Neumann WL, Salvemini D. Supraspinal peroxynitrite modulates pain signaling by suppressing the endogenous opioid pathway. The Journal of neuroscience: the official journal of the Society for Neuroscience. 2012; 32(32):10797–808. [PubMed: 22875915]
43. Schneider CA, Rasband WS, Eliceiri KW. NIH Image to ImageJ: 25 years of image analysis. Nature methods. 2012; 9(7):671–5. [PubMed: 22930834]
44. Paxinos, G.; Watson, C. The rat brain in stereotaxic coordinates. San Diego: Academic Press; 1998.
45. Livak KJ, Schmittgen TD. Analysis of relative gene expression data using real-time quantitative PCR and the 2(−Delta Delta C(T)) Method. Methods. 2001; 25(4):402–8. [PubMed: 11846609]
46. Dixon AK, Gubitz AK, Sirinathsinghji DJ, Richardson PJ, Freeman TC. Tissue distribution of adenosine receptor mRNAs in the rat. British journal of pharmacology. 1996; 118(6):1461–8. [PubMed: 8832073]
47. Shankey TV, Forman M, Scibelli P, Cobb J, Smith CM, Mills R, Holdaway K, Bernal-Hoyos E, Van Der Heiden M, Popma J, et al. An optimized whole blood method for flow cytometric measurement of ZAP-70 protein expression in chronic lymphocytic leukemia. Cytometry Part B, Clinical cytometry. 2006; 70(4):259–69.
48. Gallo-Rodriguez C, Ji XD, Melman N, Siegman BD, Sanders LH, Orlina J, Fischer B, Pu Q, Olah ME, van Galen PJ, et al. Structure-activity relationships of N6-benzyladenosine-5′-uronamides as A3-selective adenosine agonists. Journal of medicinal chemistry. 1994; 37(5):636–46. [PubMed: 8126704]
49. Tchilibon S, Joshi BV, Kim SK, Duong HT, Gao ZG, Jacobson KA. (N)-methanocarba 2, N6-disubstituted adenine nucleosides as highly potent and selective A3 adenosine receptor agonists. Journal of medicinal chemistry. 2005; 48(6):1745–58. [PubMed: 15771421]
50. Kreckler LM, Wan TC, Ge ZD, Auchampach JA. Adenosine inhibits tumor necrosis factor-alpha release from mouse peritoneal macrophages via A2A and A2B but not the A3 adenosine receptor.

The Journal of pharmacology and experimental therapeutics. 2006; 317(1):172–80. [PubMed: 16339914]

51. Wang XM, Lehky TJ, Brell JM, Dorsey SG. Discovering cytokines as targets for chemotherapy-induced painful peripheral neuropathy. Cytokine. 2012; 59(1):3–9. [PubMed: 22537849]
52. Di Cesare Mannelli L, Pacini A, Bonaccini L, Zanardelli M, Mello T, Ghelardini C. Morphologic features and glial activation in rat oxaliplatin-dependent neuropathic pain. J Pain. 2013; 14(12): 1585–600. [PubMed: 24135431]
53. Bennett GJ, Xie YK. A peripheral mononeuropathy in rat that produces disorders of pain sensation like those seen in man. Pain. 1988; 33(1):87–107. [PubMed: 2837713]
54. Hu P, Bembrick AL, Keay KA, McLachlan EM. Immune cell involvement in dorsal root ganglia and spinal cord after chronic constriction or transection of the rat sciatic nerve. Brain, behavior, and immunity. 2007; 21(5):599–616.
55. Milligan ED, Watkins LR. Pathological and protective roles of glia in chronic pain. Nature reviews. 2009; 10(1):23–36.
56. Watkins LR, Milligan ED, Maier SF. Glial proinflammatory cytokines mediate exaggerated pain states: implications for clinical pain. Adv Exp Med Biol. 2003; 521:1–21. [PubMed: 12617561]
57. Bradesi S, Eutamene H, Theodorou V, Fioramonti J, Bueno L. Effect of ovarian hormones on intestinal mast cell reactivity to substance P. Life Sci. 2001; 68(9):1047–56. [PubMed: 11212868]
58. Gao M, Yan X, Weng HR. Inhibition of glycogen synthase kinase 3beta activity with lithium prevents and attenuates paclitaxel-induced neuropathic pain. Neuroscience. 2013; 254:301–11. [PubMed: 24070631]
59. Fishman P, Bar-Yehuda S, Ohana G, Barer F, Ochaion A, Erlanger A, Madi L. An agonist to the A3 adenosine receptor inhibits colon carcinoma growth in mice via modulation of GSK-3 beta and NF-kappa B. Oncogene. 2004; 23(14):2465–71. [PubMed: 14691449]
60. Park SS, Zhao H, Jang Y, Mueller RA, Xu Z. N6-(3-iodobenzyl)-adenosine-5′-N-methylcarboxamide confers cardioprotection at reperfusion by inhibiting mitochondrial permeability transition pore opening via glycogen synthase kinase 3 beta. The Journal of pharmacology and experimental therapeutics. 2006; 318(1):124–31. [PubMed: 16611852]
61. Madi L, Cohen S, Ochayin A, Bar-Yehuda S, Barer F, Fishman P. Overexpression of A3 adenosine receptor in peripheral blood mononuclear cells in rheumatoid arthritis: involvement of nuclear factor-kappaB in mediating receptor level. J Rheumatol. 2007; 34(1):20–6. [PubMed: 17216675]
62. Varani K, Padovan M, Vincenzi F, Targa M, Trotta F, Govoni M, Borea PA. A2A and A3 adenosine receptor expression in rheumatoid arthritis: upregulation, inverse correlation with disease activity score and suppression of inflammatory cytokine and metalloproteinase release. Arthritis Res Ther. 2011; 13(6):R197. [PubMed: 22146575]
63. Varani K, Vincenzi F, Tosi A, Targa M, Masieri FF, Ongaro A, De Mattei M, Massari L, Borea PA. Expression and functional role of adenosine receptors in regulating inflammatory responses in human synoviocytes. British journal of pharmacology. 2010; 160(1):101–15. [PubMed: 20331607]
64. Hasko G, Szabo C, Nemeth ZH, Kvetan V, Pastores SM, Vizi ES. Adenosine receptor agonists differentially regulate IL-10, TNF-alpha, and nitric oxide production in RAW 264.7 macrophages and in endotoxemic mice. Journal of immunology. 1996; 157(10):4634–40.
65. Bar-Yehuda S, Luger D, Ochaion A, Cohen S, Patokaa R, Zozulya G, Silver PB, de Morales JM, Caspi RR, Fishman P. Inhibition of experimental auto-immune uveitis by the A3 adenosine receptor agonist CF101. International journal of molecular medicine. 2011; 28(5):727–31. [PubMed: 21887476]
66. Austin PJ, Kim CF, Perera CJ, Moalem-Taylor G. Regulatory T cells attenuate neuropathic pain following peripheral nerve injury and experimental autoimmune neuritis. Pain. 2012; 153(9): 1916–31. [PubMed: 22789131]
67. Moalem G, Xu K, Yu L. T lymphocytes play a role in neuropathic pain following peripheral nerve injury in rats. Neuroscience. 2004; 129(3):767–77. [PubMed: 15541898]
68. Moon HG, Tae YM, Kim YS, Gyu Jeon S, Oh SY, Song Gho Y, Zhu Z, Kim YK. Conversion of Th17-type into Th2-type inflammation by acetyl salicylic acid via the adenosine and uric acid pathway in the lung. Allergy. 2010; 65(9):1093–103. [PubMed: 20337611]

69. Ledeboer A, Jekich BM, Sloane EM, Mahoney JH, Langer SJ, Milligan ED, Martin D, Maier SF, Johnson KW, Leinwand LA, et al. Intrathecal interleukin-10 gene therapy attenuates paclitaxel-induced mechanical allodynia and proinflammatory cytokine expression in dorsal root ganglia in rats. Brain, behavior, and immunity. 2007; 21(5):686–98.

70. Madi L, Ochaion A, Rath-Wolfson L, Bar-Yehuda S, Erlanger A, Ohana G, Harish A, Merimski O, Barer F, Fishman P. The A3 adenosine receptor is highly expressed in tumor versus normal cells: potential target for tumor growth inhibition. Clin Cancer Res. 2004; 10(13):4472–9. [PubMed: 15240539]

71. Bar-Yehuda S, Stemmer SM, Madi L, Castel D, Ochaion A, Cohen S, Barer F, Zabutti A, Perez-Liz G, Del Valle L, et al. The A3 adenosine receptor agonist CF102 induces apoptosis of hepatocellular carcinoma via de-regulation of the Wnt and NF-kappaB signal transduction pathways. Int J Oncol. 2008; 33(2):287–95. [PubMed: 18636149]

72. Fishman P, Bar-Yehuda S, Barer F, Madi L, Multani AS, Pathak S. The A3 Adenosine Receptor as a New Target for Cancer Therapy and Chemoprotection. Experimental Cell Research. 2001; 269(2):230–6. [PubMed: 11570815]

73. Fishman P, Bar-Yehuda S, Madi L, Cohn I. A3 adenosine receptor as a target for cancer therapy. Anticancer Drugs. 2002; 13(5):437–43. [PubMed: 12045454]

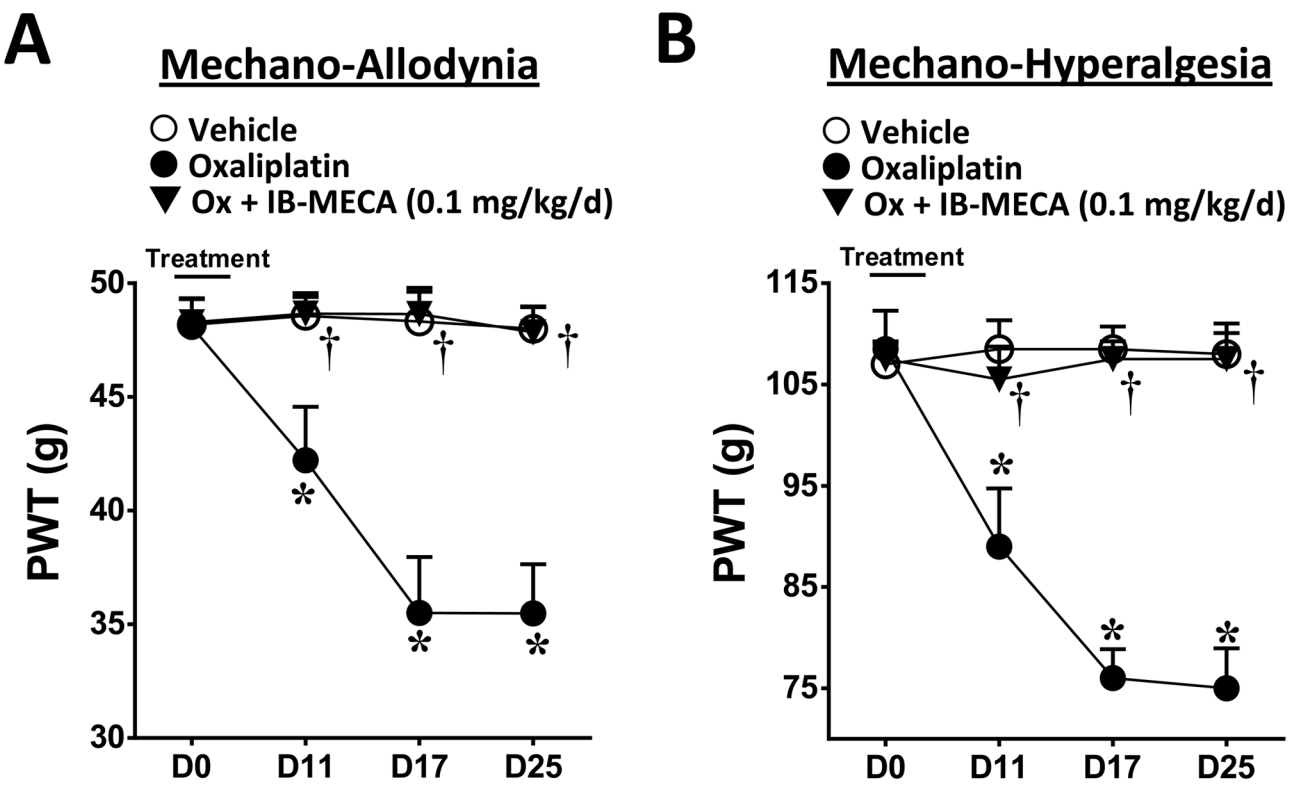

Fig. 1. Concomitant IB-MECA blocks the development of oxaliplatin-induced mechano-hypersensitivity

When compared to day (D) 0, administration of oxaliplatin (●) but not vehicle (○) led to a time-dependent development of mechano-allodynia (**A**) and mechano-hyperalgesia (**B**). The development of mechano-hypersensitivity was blocked by daily i.p. injections (D0–4) of the selective A_3AR agonist IB-MECA (0.1 mg/kg/d, ▼). The Y-axis corresponding to paw withdrawal threshold (PWT) has been cropped for clarity. *Results are expressed as mean ± SD; n=5 rats; two-way ANOVA with Bonferroni comparisons. *P<0.05 Vehicle or Oxaliplatin vs. D0; †P<0.05 Ox+IB-MECA vs. Oxaliplatin.*

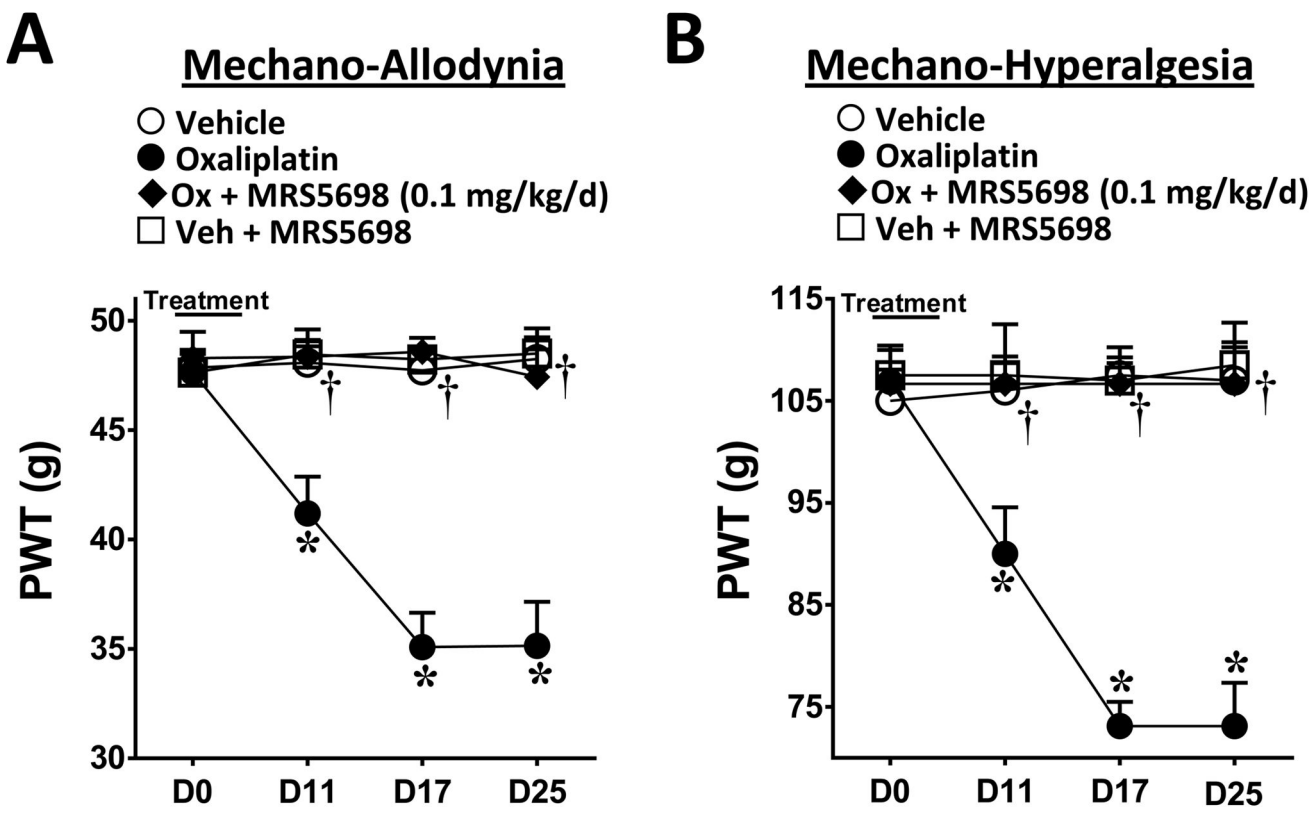

Fig. 2. MRS5698 attenuates the development of oxaliplatin-induced mechano-hypersensitivity

When compared to day (D) 0, administration of oxaliplatin (●) but not vehicle (○) led to a time-dependent development of mechano-allodynia (**A**) and mechano-hyperalgesia (**B**), which was blocked by daily i.p. injections (D0–4) with the highly selective A_3AR agonist MRS5698 (0.1 mg/kg/d, ◆). MRS5698 had no effect on vehicle-treated animals (□). The Y-axis corresponding to paw withdrawal threshold (PWT) has been cropped for clarity. *Results are expressed as mean ± SD; n=5–6 rats; two-way ANOVA with Bonferroni comparisons. *P<0.05 Vehicle or Oxaliplatin vs. D0; †P<0.05 Ox+MRS5698 vs. Oxaliplatin.*

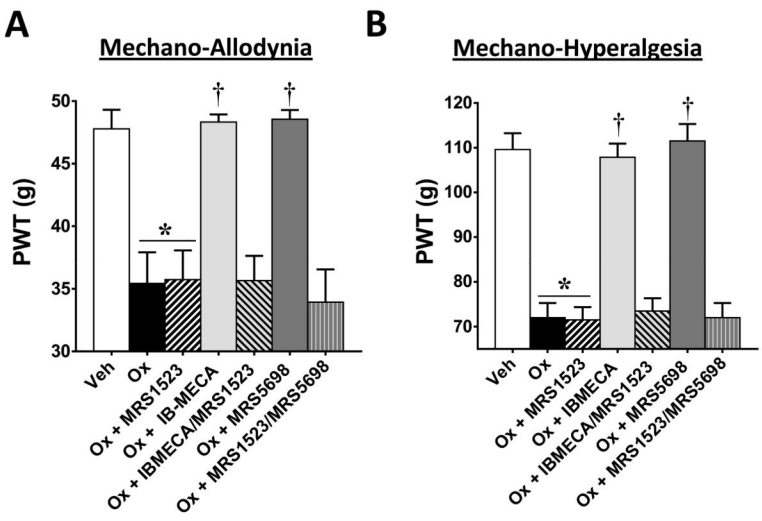

Fig. 3. MRS1523 blocks the beneficial actions of IB-MECA and MRS5698 on the development of mechano-hypersensitivity

On day (D) 25, oxaliplatin-treatment (black bars) led to the development of mechano-allodynia (**A**) and mechano-hyperalgesia (**B**) as compared to vehicle (open bars). This was blocked by daily i.p. injections (D0–4) of A_3AR agonists IB-MECA (0.1 mg/kg/d; light gray bars) or MRS5698 (0.1 mg/kg/d; dark gray bars). When MRS1523, an A_3AR antagonist, was administered prior to IB-MECA or MRS5698 (gray hatched bars), it prevented these beneficial effects (**A, B**). MRS1523 had no effect on the PWTs of oxaliplatin-treated animals when given alone (2 mg/kg/d; black hatched bars). Baselines on D0 did not significantly differ among groups. The y-axis corresponding to paw withdrawal threshold (PWT) has been cropped for clarity. *Results are expressed as mean ± SD; n=5–6 rats; one-way ANOVA with Dunnett's comparisons. *P<0.05 Oxaliplatin vs. Vehicle; †P<0.05 Ox +IB-MECA or Ox+MRS5698 vs. Oxaliplatin.*

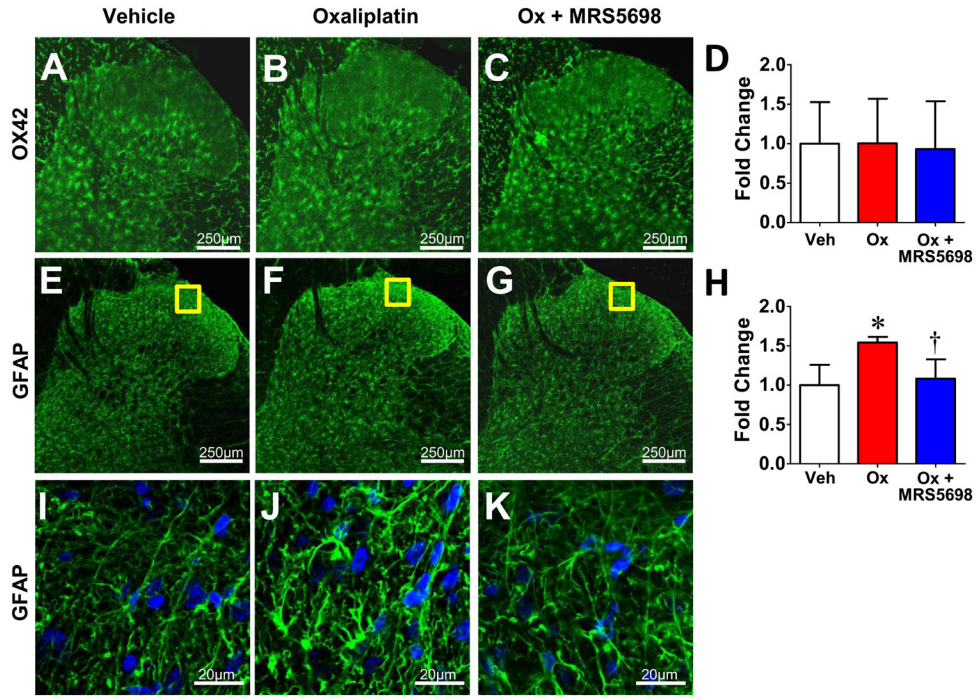

Fig. 4. MRS5698 prevents spinal astrocytic hyperactivation after oxaliplatin treatment

When compared to vehicle (**A**), oxaliplatin treated rats (**B**) at day 25 demonstrated no change in immunolabeling for OX42 (green) bilaterally within the superficial dorsal horn (i.e., laminae I and II) with (**C**) or without (**B**) MRS5698 treatment. When compared to vehicle (**E**), oxaliplatin treated rats at D25 (**F**) demonstrated enhanced immunolabeling for GFAP (green) bilaterally within the superficial dorsal horn. The A_3AR agonist MRS5698 blocked enhanced GFAP immunostaining (**G**). Negative controls exhibited low levels of background fluorescence. Micrographs are from the L4 level and represent n=4 animals per group (3 sections per animal from L4, L5, and L6). The mean fluorescence intensity (MFI) was normalized to vehicle and expressed as fold change for OX42 (**D**) and GFAP (**H**). **I–K**: Higher magnification representative images. *Results are expressed as mean ± SD and analyzed by one-way ANOVA with Dunnett's comparisons. *P<0.05 Oxaliplatin vs. Vehicle; †P<0.05 Ox+MRS5698 vs. Oxaliplatin.*

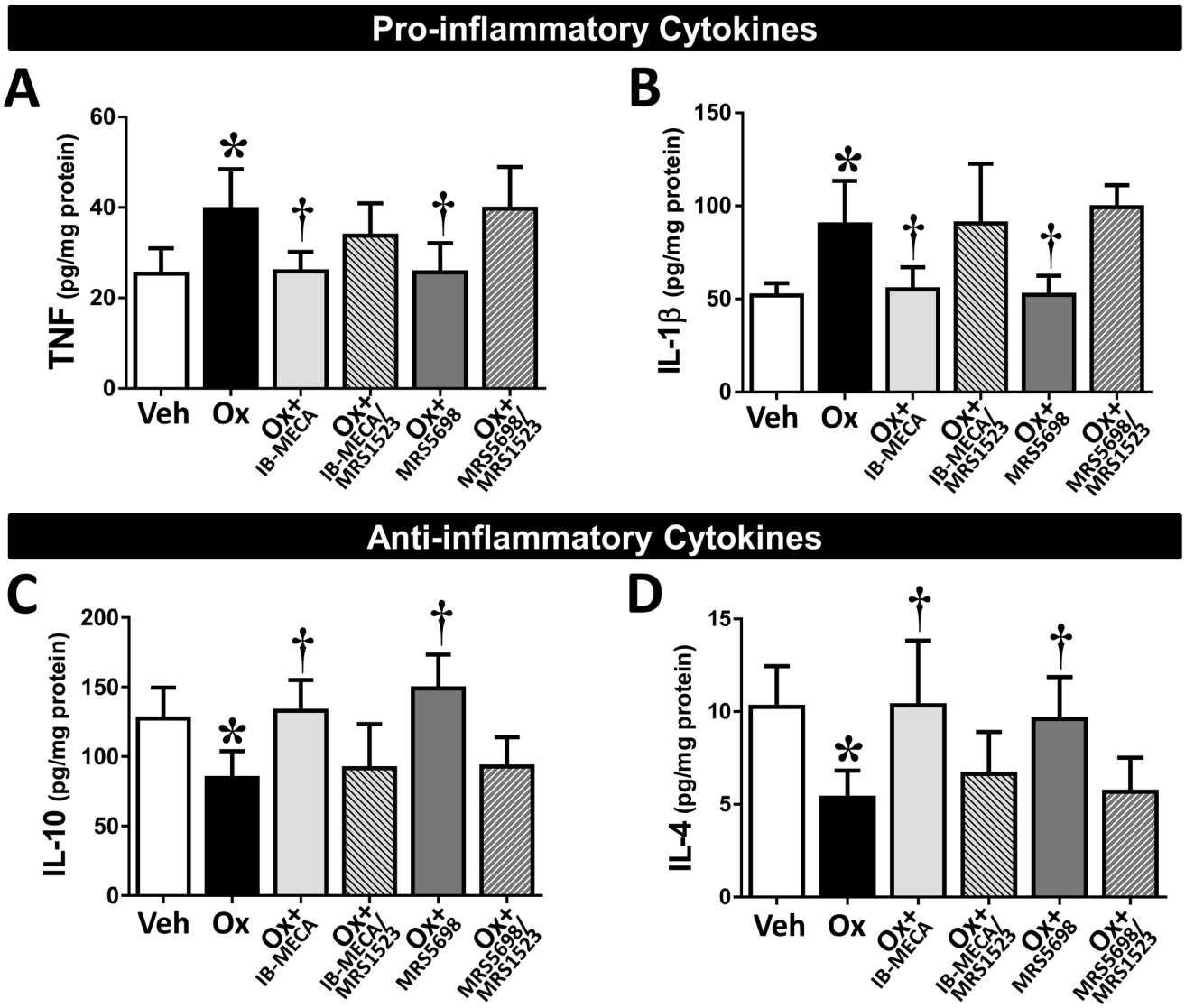

Fig. 5. IB-MECA and MRS5698 restore the balance of pro-/anti-inflammatory cytokines in the spinal cord of oxaliplatin-treated animals

On day (D) 25 of treatment, spinal cords were harvested from animals receiving vehicle (open bars), oxaliplatin (black bars), or oxaliplatin + IB-MECA (light gray bars) or + MRS5698 (dark gray bars). The spinal cord samples were assayed for levels of pro-inflammatory (TNF, **A**; IL-1β, **B**) and anti-inflammatory (IL-10, **C**; IL-4, **D**) cytokines. Selective A_3AR agonists IB-MECA and MRS5698 attenuated the increase in pro-inflammatory and decrease in anti-inflammatory cytokines observed with oxaliplatin-treatment **(A–D)**. Pretreatment with the A_3AR antagonist MRS1523 prevented the actions of both IB-MECA and MRS5698 (gray hatched bars). *Results are expressed as mean ± SD for n=5–6 and analyzed by one-way ANOVA with Dunnett's comparisons. *P<0.05 Oxaliplatin vs. Vehicle; †P<0.05 Ox+IB-MECA or Ox+MRS5698 vs. Oxaliplatin.*

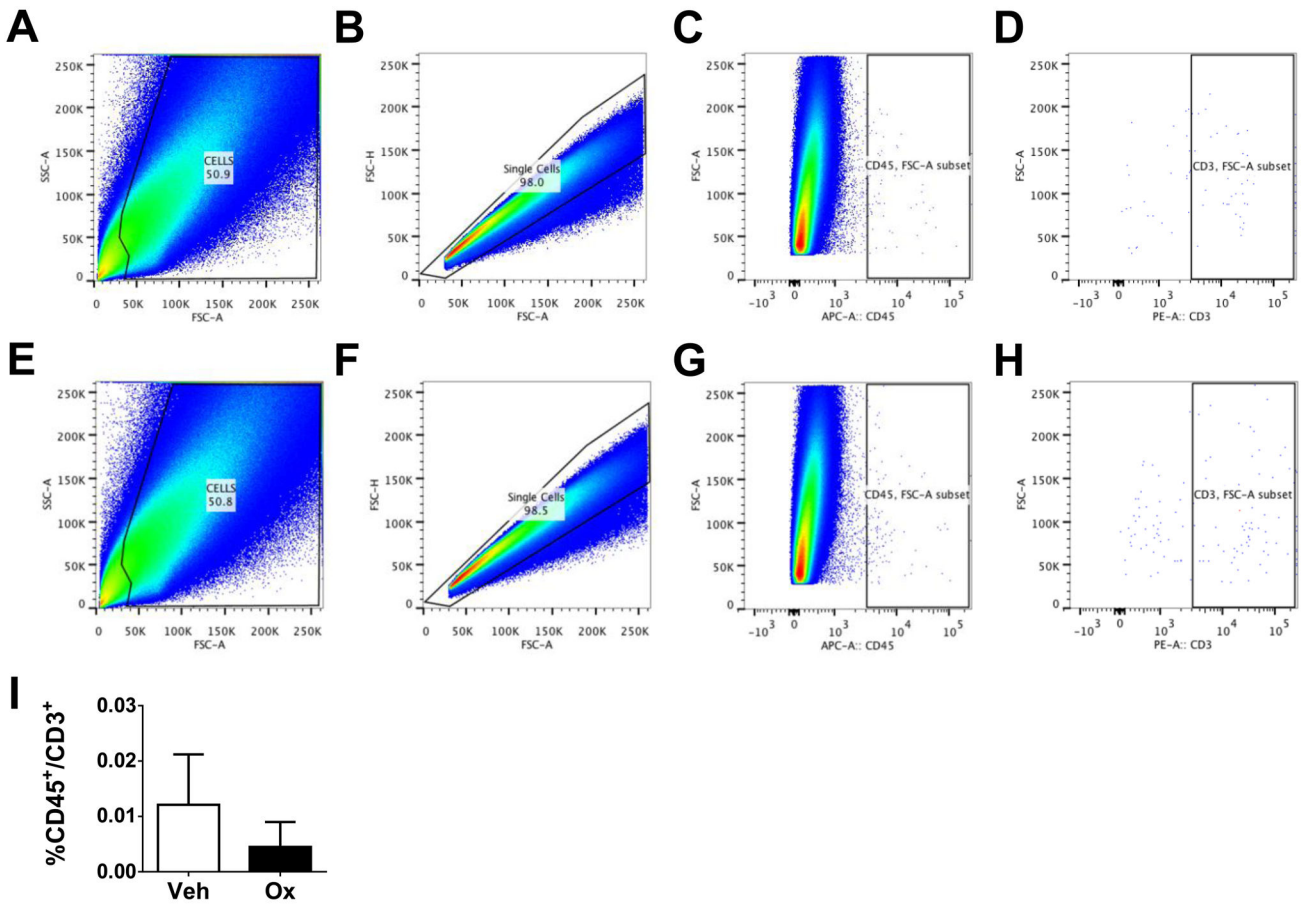

Fig. 6.

CD45/CD3 expression in the spinal cord does not change during CIPN. Flow cytometric analysis of total T-cell (CD45+/CD3+) populations show that, when compared to vehicle (A–D, I), oxaliplatin treatment (E–H, I) had no significant effect on the CD45+/CD3+ T-cell population in the dorsal lumbar spinal cord. Representative examples are shown of the scatterplots and gates used to measure the CD45+/CD3+ population (A–H). Results are expressed as mean ± SD for n=5 rats and analyzed by Student's t-test.

Table 1

CD4 expression levels in the spinal cord do not change during CIPN

No significant changes were detected in the expression levels of CD4 within the dorsal spinal cord of oxaliplatin-treated rats at a time-point of peak mechano-hypersensitivity (D25). *Results are analyzed by Student's t-test (Ct) and expressed as fold change as compared to vehicle for n=5 rats/group*.

Group	Gene	Ct (Mean ± SD)	n-value	Fold-change
Vehicle	CD4	24.4 ± 2.09	5	
	HPRT1	19.3 ± 0.200		
Oxaliplatin	CD4	23.9 ± 1.24	5	0.693
	HPRT1	19.1 ± 0.190		